

TRANSPARENT HELIUM IN STRIPPED ENVELOPE SUPERNOVAE

ANTHONY L. PIRO AND VIKTORIYA S. MOROZOVA

Theoretical Astrophysics, California Institute of Technology, 1200 E California Blvd., M/C 350-17, Pasadena, CA 91125, USA; piro@caltech.edu

Submitted for publication in The Astrophysical Journal Letters

ABSTRACT

The light curves and velocity evolution of core-collapse supernovae (SNe) provide important clues to help constrain their progenitors. This may be especially important for stripped envelope SNe (Type Ib, Ic, and I Ib), which have been elusive in providing direct connections with the massive stars that give rise to these explosions. Using simple arguments based on photometric light curves, we propose that many of these stripped envelope SNe show evidence that a significant fraction their helium is effectively transparent during the majority of their light curve evolution. This means that the helium should not contribute to the shaping of the main SN light curve and thus the total helium mass may be difficult to constrain from simple light curve modeling. Conversely, such modeling may be more useful for constraining the mass of the carbon/oxygen core of the SN progenitor. We discuss ways in which similar analysis can provide insights into the differences and similarities between SNe Ib and Ic, which will help lead to a better understanding of their respective formation mechanisms.

Subject headings: hydrodynamics — shock waves — supernovae: general

1. INTRODUCTION

Even though it has now been eighty years since the seminal work predicting that supernovae (SNe) are associated with the formation of neutron stars (Baade & Zwicky 1934), there still remains much debate on connecting the explosive events we see with their massive stellar progenitors. There is strong evidence that Type II-P SNe are the product of the core-collapse of red supergiants, both via direct identification with pre-explosion imaging (Smartt et al. 2009) and modeling of their light curves (Falk & Arnett 1977; Eastman et al. 1994; Utrobin 2007; Kasen & Woosley 2009; Dessart et al. 2010; Bersten et al. 2011; Dessart & Hillier 2011). In contrast, for the mass stripped SNe (Type Ib, Ic, and I Ib), direct identification has been more difficult with the exception of a few cases of yellow supergiants associated with SNe I Ib (Maund et al. 2011; Bersten et al. 2012). Historically, there has been some debate whether the mass stripping necessary for these events comes from the winds of effectively isolated stars or if it is due to binary interactions. However more recently, both light curve modeling (Ensmann & Woosley 1988; Dessart et al. 2011; Benvenuto et al. 2013; Bersten et al. 2014; Fremling et al. 2014), which favors relatively low ejecta masses, and the surprisingly high rate of SNe Ib and Ic (Smith et al. 2011) argue that the binary origin explains the majority of these events (also see Smith 2014).

A further complication in trying to understand the origin of mass stripped SNe is identifying the mechanism that determines whether an SN is of Type Ib or Ic. Spectroscopically, this difference is just attributed to a lack of observed helium, but as highlighted by Dessart et al. (2012), this does not necessarily mean that SNe Ic are intrinsically helium poor (although see Hachinger et al. 2012). Non-thermal excitation and ionization are key for the production of He I lines (Lucy 1991), thus an SN progenitor with helium-rich surface layers could in principle look like an SN Ib or Ic depending on the amount of mixing of ^{56}Ni . Given these complications, it would be useful to have simple rules of thumb to determine what these SNe are telling us about the presence or not of helium and understand how it impacts other inferences about the

progenitor. This is the motivation of the present work.

A further motivation is the steadily growing sample of stripped envelope SNe being discovered by current and future surveys and efforts to collect SNe, such as PTF (Rau et al. 2009), Pan-STARRS (Kaiser et al. 2002), CSP (Hamuy et al. 2006), LCOGT (Brown et al. 2013), ZTF (Law et al. 2009), ASAS-SN (Shappee et al. 2013), and LSST (LSST Science Collaboration et al. 2009). This allows events to be studied in aggregate to search for interesting trends in the ejecta masses, energetics, ^{56}Ni , and a range of other properties (Lyman et al. 2014). Such work is well-suited for simple modeling to control the parameter space, but it is only useful if the limitations of such modeling are properly understood.

In Section 2, we summarize simple arguments demonstrating that the He I lines in at least some SNe Ib are a useful tracer for the photosphere. This demonstrates that we are likely seeing deep into the SN ejecta. This is compared with hydrodynamic models of exploding stars to strengthen this case. Coupled with the temperature evolution presented in Section 3 and the opacity of the helium-rich surface layers, we argue that a non-negligible fraction of helium is recombined in these events. We conclude in Section 4 with a summary of our conclusions and a discussion of future work, particularly for comparing Type Ib and Ic SNe.

2. COLOR VELOCITY EVOLUTION

As a shock passes through an exploding star, it accelerates and unbinds the material. The velocity to which the ejecta is accelerated can vary greatly throughout the star and is sensitive to the stellar density profile as described in Matzner & McKee (1999). Roughly speaking, the velocity decreases as the shock moves out and sweeps up more mass, but it can also accelerate in regions where the density decreases rapidly, such as at the surface of the star or at the edges of burning shells. In principle, the observed velocities of the ejecta should encode information about the progenitor structure in this way.

This can be seen in Figure 1, which shows in the upper panel the terminal velocity profile, for a range of different explosion energies, in a star that has a mass of $\sim 5 M_{\odot}$ at the moment of core collapse. This star was generated from a $15 M_{\odot}$

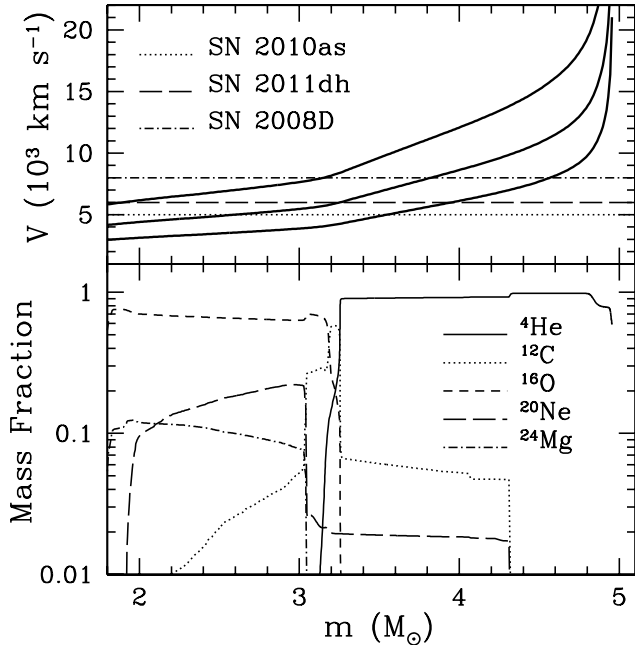


FIG. 1.— The profile of an exploding star as a function of mass coordinate. The model is a $15M_{\odot}$ zero-age main-sequence star with its hydrogen envelope removed to simulate mass loss in a binary system. The upper panel shows the terminal velocity profile of 10^{51} , 2×10^{51} , and 4×10^{51} erg explosions (solid lines, from bottom to top). The horizontal lines show typical He I velocities for each of the studied SNe near peak luminosity to help guide the eye. The bottom panel shows the composition of the most abundant elements at the moment of core-collapse.

zero-age main-sequence star using the 1D stellar evolution code MESA (Paxton et al. 2013). Using the overshooting and mixing parameters recommended by Sukhbold & Woosley (2014), the star is evolved until a large entropy jump between the core and envelope was established. The entire convective envelope is removed to mimic mass loss during a common envelope phase, and then the star continues to evolve up to the onset of core collapse. A shock is initiated by heating the star at a mass coordinate of $m = 1.5M_{\odot}$, and the subsequent hydrodynamics evolution is followed using our 1D Lagrangian supernova explosion code (SNEC, Morozova et al. in preparation, which follows the numerical hydrodynamic scheme of Mezzacappa & Bruenn 1993). The main features to note are the great acceleration of the shock near the surface and the more modest acceleration at the boundary between the carbon/oxygen layers and the helium-rich surface layers. In the bottom panel of Figure 1, we plot the composition of some of the most abundant elements in the star prior to explosion.

In recent work by Folatelli (2014), it was pointed out that some SNe Ibc appear to have anomalously low He I velocities in the range of 4,000 to 8,000 km s^{-1} with one of the prime examples being SN 2010as (see Figure 2). This is lower than the typical velocities of 10,000 to 15,000 km s^{-1} (see the surface layers in Figure 1) typically associated with the photosphere. In addition, the evolution with time is much flatter, which is again not expected given the high velocity gradient in the surface layers.

To better understand what is implied by these seemingly low velocities, it is helpful to consider the velocity of material at the color depth in the star as a function of time, henceforth referred to as the color velocity. For a black body with temperature T_{BB} and color radius r_c , the bolometric luminosity is

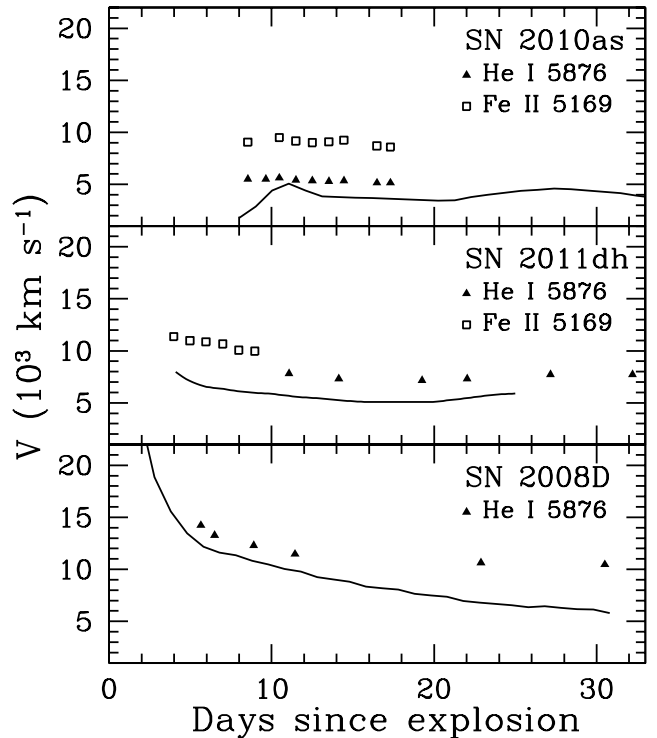


FIG. 2.— The solid line in each case marks V_c in the SN that was found using Equation (1). The upper two panels are Type IIb SNe that have been noted for their especially low velocity helium, while the bottom panel is a SN Ib with a more typical velocity evolution. Nevertheless, in all three cases, the velocity of the color depth is below the helium velocity.

$L = 4\pi r_c^2 \sigma_{\text{SB}} T_{\text{BB}}^4$, where σ_{SB} is the Stefan-Boltzmann constant. Substituting $r_c = V_c t$, where V_c is the color velocity,

$$V_c = \frac{1}{t} \left(\frac{L}{4\pi \sigma_{\text{SB}} T_{\text{BB}}^4} \right)^{1/2}. \quad (1)$$

The color radius r_c is roughly where an incoming photon would experience at least one absorption, rather than just a scattering, and thus where the observed black body temperature is determined (see Nakar & Sari 2010). The color radius is in general slightly deeper than the actual photosphere. Nevertheless, V_c should provide a useful diagnostic for roughly tracking the photospheric velocity.

Equation (1) is used to analyze three different events, the Type IIb SNe 2010as (Folatelli 2014) and 2011dh (Marion et al. 2014), and the Type Ib SN 2008D (Modjaz et al. 2009). Although SNe IIb have a thin hydrogen layer at the surface (Woosley et al. 1994; Bersten et al. 2012; Nakar & Piro 2014), this is sufficiently low mass that it will be optically thin at the times we consider and not affect our arguments. All three are shown in Figure 2, along with the measured He I 5876 absorption line velocity and in two cases the Fe II 5169 velocity. Strikingly, in all three cases, V_c is similar but less than the helium velocity. This argues that indeed the helium is tracking the photosphere, and that even when the velocity is low there is nothing intrinsically anomalous about the helium. Rather this is simply consistent with the velocity of the ejecta as inferred from the luminosity and temperature.

As a comparison, in the upper panel of Figure 1 we also plot horizontal lines that roughly show V_c for each event near peak luminosity. In each case, V_c is not dissimilar to what is

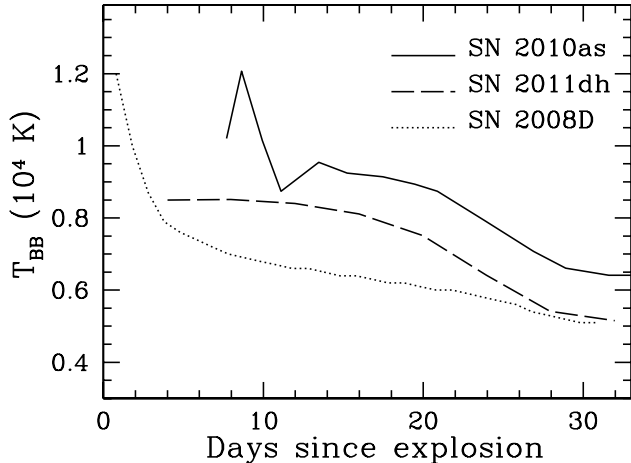


FIG. 3.— Black body temperature as a function of time for each of the three SNe, using the data from Folatelli (2014), Marion et al. (2014), and Modjaz et al. (2009).

expected near the boundary between the carbon/oxygen inner layers and the more helium-rich surface layers. Furthermore, one can see that the velocity profile near these regions is much shallower than the surface velocity, again consistent with what is observed for the He I features. Although this comparison cannot provide a quantitative result, at least qualitatively it appears we are looking deep into the ejecta.

3. TEMPERATURE AND OPACITY

To understand why the helium is appearing as it is, it is helpful to consider the actual black body temperatures that are being observed. In Figure 3, we plot the temperature evolution for each of the three SNe. In comparison, in Figure 4, we plot the opacity as a function of temperature for helium-rich material (Badnell et al. 2005, and references therein), as is expected in the outer layers of these stripped envelope progenitors. Above a temperature of $\approx 10^4$ K, the opacity is $\approx 0.1 \text{ cm}^2 \text{ g}^{-1}$, consistent with electron scattering from material with one electron per four nucleons (i.e., singly ionized helium). Below this temperature, the opacity is almost zero and the material is effectively transparent. We also consider a mixture with 10% carbon and oxygen to demonstrate how robust this feature is. This particular plot uses a density of $10^{-11} \text{ g cm}^{-3}$, but the threshold at which this happens is not strongly dependent on density. Only once the material is largely carbon/oxygen does the opacity increase much for $T \lesssim 1.2 \times 10^4$ K. Thus the photosphere is deep within the helium layer ($\sim 1 M_\odot$ or more) and potentially as far as the interface between the carbon/oxygen and helium-rich material.

Comparing Figures 3 and 4, it seems unavoidable to conclude that a large fraction of helium in these events is transparent. To be clear, it is true that helium absorption lines are seen in all of these SNe, but this is only at a few specific wavelengths. What we are arguing is that across the majority of the spectrum, the helium-rich material is not drastically impacting the time it takes photons to diffuse out of the expanding ejecta of the SN. This has important implications for studies that wish to use simple models to constrain the properties of the SNe from their photometric light curves. The basic idea of these works is to effectively use the diffusion time through the ejecta (Arnett 1982) to relate the rise time of the SN to the ejecta mass, $t_{\text{rise}} \propto (\kappa M_{\text{ej}} / v_{\text{ej}} c)^{1/2}$, where M_{ej} and v_{ej} are

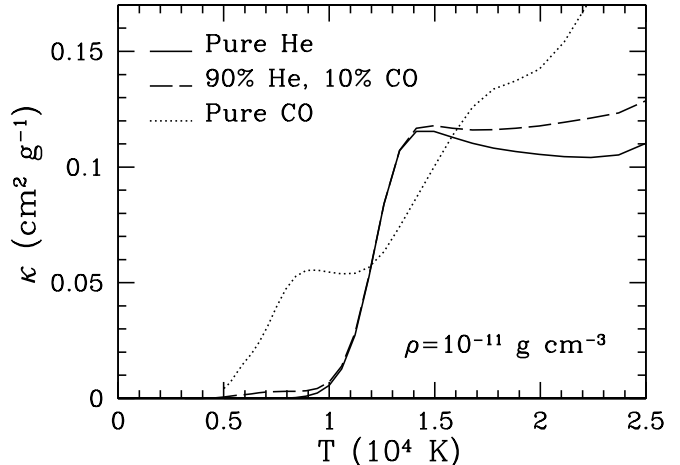


FIG. 4.— The Rosseland mean opacity as a function of temperature and a representative density of $10^{-11} \text{ g cm}^{-3}$ (κ is weakly dependent on density). We plot a composition of pure helium (solid line), helium with a 10% mass fraction carbon/oxygen (dashed line), and pure carbon/oxygen (dotted line).

the typical mass and velocity of the ejecta, respectively. This should work as long as the opacity κ is representative of the majority of the material, but not if κ varies by a large amount as happens if some material is transparent.

Recently Lyman et al. (2014) used similar semi-analytic methods to study the ejecta mass in 38 Type IIb, Ib, Ic, and Ic-BL SNe. One particularly striking conclusion was that the majority of these stripped envelope SNe have rather similar ejecta masses in the range of $\sim 1 - 5 M_\odot$. If the typical understanding of the difference between SNe Ib and Ic were true, namely that SNe Ic have additional mass loss to remain their helium envelopes, one would instead expect on average larger ejecta masses from SNe Ib. Our discussion here demonstrates that indeed the SNe Ib could have more ejecta overall, but the mass of the helium does not impact the light curve width because it is transparent. Conversely, the Lyman et al. (2014) study is constraining the ejecta mass of high opacity material, which, as we show in Figure 4, must have a significant fraction of carbon/oxygen. *We conclude that what these studies are roughly measuring is the mass of the carbon/oxygen core.* If this is the case, then it is natural that the inferred ejecta mass is similar, independent of the amount of helium stripping.

One potential complication is if there are opacity sources not taken into account in Figure 4 that increase the opacity even when helium is recombined. A standard practice for hydrodynamic codes that use a Rosseland mean opacity is to invoke an opacity floor (Bersten et al. 2011, and references therein). This is meant to replicate things like bound-free and bound-bound absorptions, and non-thermal excitation or ionization of electrons by Compton scattering of γ -rays (although Kleiser & Kasen 2014 show that at least the bound-bound opacity for pure-helium is negligible). Nevertheless, the close match between the He I line velocities and V_c in Figure 2 argues that this opacity floor cannot be too large and that a non-negligible fraction of the helium is recombined and not providing a large opacity. This conclusion should be checked with future Rosseland mean opacity calculations of helium-rich mixtures at low temperatures.

4. CONCLUSION AND DISCUSSION

In this work, we have inferred the time-dependent color velocity V_c for three different SNe and demonstrated in each

case that it is below the lowest velocity He I absorption features. Coupled with (1) the $\lesssim 10^4$ K black body temperature observed for all of these events, (2) the typical threshold of 1.2×10^4 K for helium ionization, and (3) comparisons to the velocity profiles in hydrodynamic models of mass stripped stars, this all suggests that a non-negligible amount of helium is effectively transparent during these events. As described above, this could in principle result in a solar mass or more of material being missed by simple models attempting to infer the ejecta mass. *Even in detailed numerical studies of these events, constraining the total ejecta mass may be difficult.* This is because even if a given model is shown to fit, a similarly good fit may also be possible with an additional amount of helium. Future numerical modeling needs to quantify just how much helium can actually be hidden.

These results will hopefully motivate similar analysis of V_c in future SN studies. This has recently been done for the SN Ib iPTF13bvn (Fremming et al. 2014), and again the temperatures are well below 10^4 K and V_c is similar but slightly below the lowest velocity helium features. An important conclusion of this work was that the ejecta mass was constrained to be $\approx 2M_\odot$ (also see Bersten et al. 2014, who find a similar ejecta mass), and thus clearly rules out a Wolf-Rayet progenitor which would have $\sim 8M_\odot$ or more of ejecta at the time of core collapse. Although transparent helium may not be enough to reconcile this ejecta mass difference with a Wolf-Rayet star, it could easily be a significant correction.

To maximize the usefulness of these future studies, it will be important to have measurements of L , T_{BB} , and t , so that Equation (1) can be properly used. This puts particular emphasis on covering all wavelengths so that the bolometric luminosity and black body temperature can be accurately inferred (see the discussion in Marion et al. 2014). Infrared can be especially helpful for correctly inferring the He I velocities since at optical wavelengths He I absorption features can potentially be confused with other elements (although in any case the lowest securely observed He I velocity should always be used to get as close to the photosphere as possible). Get-

ting an accurate t requires that the SN be detected as early as possible after the explosion, since in cases where a first peak in the light curve is not seen it can be difficult to know exactly when the explosion happened (Piro & Nakar 2013).

Comparing and contrasting this type of analysis between SNe Ib and Ic may be especially instructive for understanding their respective origins. The SN shock will always accelerate surface material to velocities of $\approx 10,000 - 15,000 \text{ km s}^{-1}$ near the surface of the star, as shown in Figure 1. If SNe Ic are truly devoid of helium, then these large velocities will occur in higher opacity carbon/oxygen material rather than lower opacity helium material. This should give rise to $V_c \approx 10,000 - 15,000 \text{ km s}^{-1}$ with a larger velocity gradient. If transparent or partially transparent helium is inferred to be present in all SNe Ib while SNe Ic show V_c evolution that is consistent with no helium present, *this would be strong evidence that SNe Ic experience more mass stripping than SNe Ib.* Such comparisons would also be useful between the various subclasses of envelope stripped SNe, such as Types Ib, Ic, IIb, and Ic-BL. If instead there is evidence for transparent helium in both Type Ib and Ic SNe, this would strongly argue that the relative deposition of helium versus ^{56}Ni is helping to determine the classification, as described by Dessart et al. (2012). In this case, issues like mixing, turbulence, rotation, and asymmetries need to more fully considered for generating a Type Ib or Ic. No matter the solution, determining between these scenarios would be an important step forward for our understanding of stripped envelope SNe.

We thank Drew Clausen for generating the $15M_\odot$ model used for Figure 1, Mattias Ergon for helpful discussions, and Dan Kasen and Christian Ott for feedback on previous drafts. We also thank the Carnegie Supernova Project, and in particular Mark Phillips, for generously hosting ALP at the CSP II Team Meeting at St. George Island, Florida where this work was inspired. This work was supported through NSF grants AST-1205732, PHY-1068881, PHY-1151197, PHY-1404569, and the Sherman Fairchild Foundation.

REFERENCES

- Arnett, W. D. 1982, *ApJ*, 253, 785
 Baade, W., & Zwicky, F. 1934, *Proceedings of the National Academy of Science*, 20, 254
 Badnell, N. R., Bautista, M. A., Butler, K., et al. 2005, *MNRAS*, 360, 458
 Benvenuto, O. G., Bersten, M. C., & Nomoto, K. 2013, *ApJ*, 762, 74
 Bersten, M. C., Benvenuto, O., & Hamuy, M. 2011, *ApJ*, 729, 61
 Bersten, M. C., Benvenuto, O. G., Nomoto, K., et al. 2012, *ApJ*, 757, 31
 Bersten, M. C., Benvenuto, O. G., Folatelli, G., et al. 2014, *ArXiv e-prints*, arXiv:1403.7288
 Brown, T. M., Baliber, N., Bianco, F. B., et al. 2013, *PASP*, 125, 1031
 Dessart, L., & Hillier, D. J. 2011, *MNRAS*, 410, 1739
 Dessart, L., Hillier, D. J., Li, C., & Woosley, S. 2012, *MNRAS*, 424, 2139
 Dessart, L., Hillier, D. J., Livne, E., et al. 2011, *MNRAS*, 414, 2985
 Dessart, L., Livne, E., & Waldman, R. 2010, *MNRAS*, 408, 827
 Eastman, R. G., Woosley, S. E., Weaver, T. A., & Pinto, P. A. 1994, *ApJ*, 430, 300
 Ensmann, L. M., & Woosley, S. E. 1988, *ApJ*, 333, 754
 Falk, S. W., & Arnett, W. D. 1977, *ApJS*, 33, 515
 Folatelli, G. 2014, in *IAU Symposium*, Vol. 296, *IAU Symposium*, ed. A. Ray & R. A. McCray, 340–341
 Fremming, C., Sollerman, J., Taddia, F., et al. 2014, *A&A*, 565, A114
 Hachinger, S., Mazzali, P. A., Taubenberger, S., et al. 2012, *MNRAS*, 422, 70
 Hamuy, M., Folatelli, G., Morrell, N. I., et al. 2006, *PASP*, 118, 2
 Kaiser, N., Aussel, H., Burke, B. E., et al. 2002, in *Society of Photo-Optical Instrumentation Engineers (SPIE) Conference Series*, Vol. 4836, *Survey and Other Telescope Technologies and Discoveries*, ed. J. A. Tyson & S. Wolff, 154–164
 Kasen, D., & Woosley, S. E. 2009, *ApJ*, 703, 2205
 Kleiser, I. K. W., & Kasen, D. 2014, *MNRAS*, 438, 318
 Law, N. M., Kulkarni, S. R., Dekany, R. G., et al. 2009, *PASP*, 121, 1395
 LSST Science Collaboration, Abell, P. A., Allison, J., et al. 2009, *ArXiv e-prints*, arXiv:0912.0201
 Lucy, L. B. 1991, *ApJ*, 383, 308
 Lyman, J., Bersier, D., James, P., et al. 2014, *ArXiv e-prints*, arXiv:1406.3667
 Marion, G. H., Vinko, J., Kirshner, R. P., et al. 2014, *ApJ*, 781, 69
 Matzner, C. D., & McKee, C. F. 1999, *ApJ*, 510, 379
 Maund, J. R., Fraser, M., Ergon, M., et al. 2011, *ApJ*, 739, L37
 Mezzacappa, A., & Bruenn, S. W. 1993, *ApJ*, 405, 669
 Modjaz, M., Li, W., Butler, N., et al. 2009, *ApJ*, 702, 226
 Nakar, E., & Piro, A. L. 2014, *ApJ*, 788, 193
 Nakar, E., & Sari, R. 2010, *ApJ*, 725, 904
 Paxton, B., Cantiello, M., Arras, P., et al. 2013, *ApJS*, 208, 4
 Piro, A. L., & Nakar, E. 2013, *ApJ*, 769, 67
 Rau, A., Kulkarni, S. R., Law, N. M., et al. 2009, *PASP*, 121, 1334
 Shappee, B. J., Prieto, J. L., Grupe, D., et al. 2013, *ArXiv e-prints*, arXiv:1310.2241
 Smartt, S. J., Eldridge, J. J., Crockett, R. M., & Maund, J. R. 2009, *MNRAS*, 395, 1409
 Smith, N. 2014, *ArXiv e-prints*, arXiv:1402.1237
 Smith, N., Li, W., Filippenko, A. V., & Chornock, R. 2011, *MNRAS*, 412, 1522
 Sukhbold, T., & Woosley, S. E. 2014, *ApJ*, 783, 10
 Utrobin, V. P. 2007, *A&A*, 461, 233
 Woosley, S. E., Eastman, R. G., Weaver, T. A., & Pinto, P. A. 1994, *ApJ*, 429, 300